ELSEVIER

International Journal of Mass Spectrometry 221 (2002) 93–105

International Journal of Mass Spectrometry

www.elsevier.com/locate/ijms

Structure characterization of petroleum vacuum residues by in-beam EI Fourier transform ion cyclotron resonance mass spectrometry

Keiko Miyabayashi*, Yasuhide Naito, Kazuo Tsujimoto, Mikio Miyake

School of Materials Science, Japan Advanced Institute of Science and Technology (JAIST), 1-1 Asahidai, Tatsunokuchi, 923-1292 Ishikawa, Japan

Received 10 April 2002; accepted 9 August 2002

Abstract

A *n*-heptane soluble fraction (AH-VR-Sa) of Arabian heavy vacuum residues (AH-VR) has been analyzed by in-beam electron ionization Fourier transform ion cyclotron resonance mass spectrometry (EI FT-ICR MS). The probe temperature and the ionization energy of in-beam EI were independently adjusted to expand the detectable range of peaks originating from components of AH-VR-Sa and to prevent fragmentation of the molecular ions. The upper mass limit of the peaks was extended to $m/z = 700$ when the probe temperature and the ionization energy were set to 300 °C and 30 eV, respectively. The average molecular weight of the spectrum increased by an increase in the probe temperature. The molecular formulas of compounds in AH-VR-Sa were determined essentially based on accurate mass measurements. Major components of being characterized were hydrocarbons both with and without one sulfur atom. The compound type estimated on the basis of hydrogen-deficiency index Z (C_nH_{2n+Z}) was discussed. The strongest peaks of hydrocarbons with sulfur atom showed the Z value of -10. The compound type analysis indicates that sulfur atom may be located at an aromatic ring but not at a side chain. The effect of experimental conditions on the detectable compound type distribution was also discussed. The present results demonstrate that the characterization of vacuum residues by in-beam EI FT-ICR MS is advantageous over the conventional EI FT-ICR MS in the detectable range of peaks and in the versatility for samples. In-beam EI FT-ICR MS is useful as a complementary method to characterize vacuum residues by electrospray ionization (ESI) FT-ICR MS, since ESI cannot ionize hydrocarbons with high Z values. (Int J Mass Spectrom 221 (2002) 93–105)

Keywords: FT-ICR; In-beam EI; Vacuum residue; Complex mixture analysis

1. Introduction

Vacuum residues are extremely complex mixtures of thousands of non-polar compounds [1,2]. Conventionally, double focusing mass spectrometry has been used to analyze the compound type distributions of constituent molecules [3–5]. The mass scale requires trimming down to narrow segments for achieving high resolution and repeating the measurements to cover a desirable mass range due to a limit of the mass resolving power. Prevalence of high magnetic field FT-ICR MS may facilitate the molecular level

* Corresponding author. E-mail: keiko@jaist.ac.jp

1387-3806/02/$ – see front matter
PII S1387-3806(02)00897-7

characterization of complex mixture across the whole mass range at once because of its high-resolution and high-sensitivity.

Several research groups have applied FT-ICR MS to analyze constituents in petroleum distillates, diesel fuel or heavy crude oil [6–11]. EI is an effective means for generating ions of both aliphatic and aromatic hydrocarbons whether with or without hetero atoms (sulfur, oxygen and/or nitrogen) in the gas phase. FT-ICR MS with 3 T superconducting magnet was used to analyze a crude oil fraction by Guan et al. [7] and a virgin vacuum gas oil by Hsu et al. [6]. Both groups had difficulty in achieving high-resolution measurements over the full mass range due to the mass resolving power available at the relatively low magnetic field strength; it was still necessary to analyze a small segment of the mass range at a time. Rodgers et al. had improved the resolving power of the FT-ICR by increasing the magnetic field to 5.6 T and reported a compositional analysis of raw diesel fuel [8]. An all-glass heated inlet system was used for injecting the petrochemical sample and objecting a relatively low-boiling fraction which should be detected in the range of $90 < m/z < 300$. Although FT-ICR MS can perform high-resolution measurement, it is still a challenge to characterize petroleum distillate in molecular level because of its extreme complexity.

EI is generally difficult to generate molecular ions from non-volatile samples. Application of EI essentially forms fragment ions because thermal decomposition occurs preference to sample vaporization. Ohashi et al. modified an EI probe to in-beam EI and successfully detected molecular ions of non-volatile samples such as oligosaccharides [9].

ESI is promising method to ionize non-volatile samples such as a high-boiling fraction of petroleum distillate, particularly when it is coupled with FT-ICR MS [10–12]. Barkel and coworkers reported that poly-condensed aromatic compounds with low ionization potential were ionized by ESI in the presence of an electron acceptor, such as 2,3-dichloro-5, 6-dicyano-1,4-benzoquinone or SbF_5 [13,14]. In our preliminary application of ESI FT-ICR MS to determine molecular formulas of constituents in Arabian mix vacuum residue (AM-VR) without any pre-separation procedures, poly-condensed aromatic homologues ($Z \leq -10$) were detected [10]. These assignments were recently improved by considering attribution of nitrogen-containing aromatic compounds, whose Z values were ranging from -12 to -44. Our observation together with the elemental composition of AM-VR implies that only partial constituents might be detected under the ESI conditions. This possibility was supported by a recent ESI FT-ICR MS analysis of heavy crude oil by Qian et al., detecting almost exclusively nitrogen-containing aromatic compounds with Z values ranging from -5 to -29 [12]. In addition, we have detected no peaks in the application of ESI FT-ICR MS to AH-VR-Sa, while in-beam EI to AH-VR gave the peaks. These facts insist that in-beam EI could be a prospective ionization technique alternative to ESI for analysis of vacuum residue.

This paper describes estimation of the preferable in-beam EI conditions to characterize the components in vacuum residue by the coupling of FT-ICR MS. We have examined the experimental conditions to detect large molecular ions and to prevent from fragmentation. Constituents in AH-VR-Sa were characterized and the structural features were discussed.

2. Experimental methods

2.1. Sample preparation

Arabian heavy vacuum residue (AH-VR) with a higher boiling point than 520 °C was used as a sample. The AH-VR sample was extracted with *n*-heptane under reflux then maltene (soluble fraction) and asphaltene (insoluble fraction) were obtained. The maltene was subsequently separated by alumina column chromatography. The fractions eluted by *n*-heptane, toluene, and toluene/methanol/chloroform were defined as AH-VR-Sa, AH-VR-Ar and AH-VR-Re, respectively. In sample preparation for mass measurements, the each fraction (1 mg) was dissolved in 1 mL of methylene chloride. 0.5 μL of the each sample solution was loaded on the in-beam EI probe tip.

2.2. In-beam EI FT-ICR MS

A commercial probe was modified for in-beam EI. To put the sample near the tungsten filament, platinum wire (15 mm in length, 1.1 mm in diameter) was inserted into a platinum vial. The distance from the end of the platinum wire to the filament is around 1 cm. The wire can be heated up to 350 °C. The probe temperature and the ionization energy were independently changed from 150 to 350 °C and from 20 to 70 eV to evaluate the best experimental conditions. The measurements were performed with a Bruker BioAPEX II FT-ICR mass spectrometer, equipped with a 7 T superconducting magnet and an external EI source. Each spectrum was acquired by accumulating 32 scans of time-domain transient signals in the length of 256k points. The extraction voltage of ion source was set to −6.6 V. The ionization pulse length was set to 50 ms. The source housing temperature was maintained at 150 °C to assist vaporization of the samples and prevent them from sticking on. All spectra were detected in the positive ion mode.

2.3. Calibration and assignment

Perfluorotri-*n*-buthyl amine was used as an internal reference for calibrating the mass scale. This calibrant was introduced into source chamber through the liquid inlet system at 90 °C located on the external ion source. Molecular formula determination was carried out with ‘mass analysis’ which is a function of XMASS software. Kendrick mass scale was also used to confirm enormous amount of calculated molecular formulas and to sort out the components in each compounds series [15].

3. Results and discussion

3.1. Estimation of optimum experimental conditions of in-beam EI FT-ICR MS for AH-VR-Sa

The mass spectra of AH-VR-Sa measured under various ionization energies from 30 to 70 eV and fixed probe temperature at 200 °C are shown in Fig. 1. No

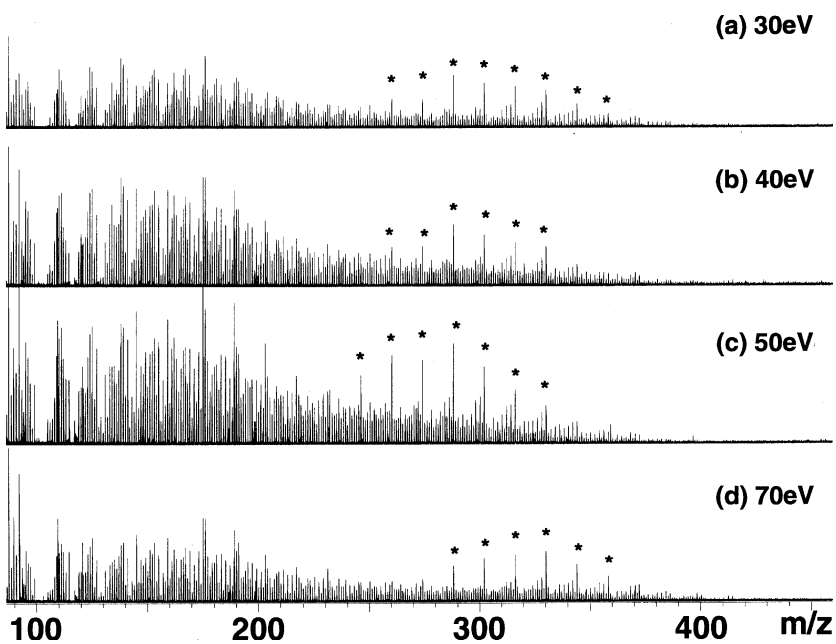

Fig. 1. Effect of ionization energy of in-beam EI on FT-ICR mass spectrum for AH-VR-Sa. The ionization energies were set to (a) 30 eV, (b) 40 eV, (c) 50 eV, and (d) 70 eV, respectively.

peaks were detected when the ionization energy was below 30 eV. Almost 600 distinguishable peaks originating from components of AH-VR-Sa were observed up to around *m*/*z* 400 for every spectrum in Fig. 1. These spectra show a bimodal distribution with mode *m*/*z* values at around 150 and 300. A similar bimodal distribution was reported for the maltene fraction of Furrial crude oil by APCI [16]. Thus, the most probable reason of the observed bimodal distribution may originate from the constituents of AH-VR-Sa, the maltene fraction of AH-VR. The peak intensities increased over the whole detected range as raising the ionization energy up to 50 eV, then decreased at 70 eV. Possibly, the decrease in peak intensities at 70 eV may be due to the dimension and structure of the ionization source block of our instrument because we often observed the similar tendency in other samples. By an increase in the ionization energy from 30 to 50 eV, the distribution of a series of prominent peaks (∗) and a myriad of tiny peaks shifted toward low mass and high mass region, respectively. For exploring the change in spectral distribution depending on the ionization energy, the obtained spectra were segmented into every 50 Da mass window and the total peak intensities of each segment were plotted in the normalized scale (Fig. 2). In the low *m*/*z* windows ($150 < m/z < 250$) the relative intensities showed the maximum at the ionization energy of 50 eV. On the other hand, those in the high *m*/*z* windows ($300 < m/z < 400$) showed almost the minimum at 50 eV. The tendency observed in the low *m*/*z* windows may reflect the enhanced degree of fragmentation under higher ionization energy. Thus, we estimated that the fragmentation was minimized at the lowest ionization energy of 30 eV. Another possibility is the difference in ionization efficiency depending on the different structures of various constituents in AH-VR-Sa. The high peak intensity was observed in the high mass window exceeding *m*/*z* 300 at the high ionization energy of 70 eV. This may suggest the diversity of ionization efficiency: some constituent with high molecular weights ionized over 70 eV. It should be mentioned that vacuum residues are extremely complex mixtures of different chemical species which will be ionized at different ionization energies. The constituents which were ionized at the different ionization energies will be discussed later.

The effects of probe temperature on mass spectra of AM-VR-Sa were examined to estimate suitable conditions. The segmented mass spectra obtained under various probe temperature from 150 to 350 °C and at the fixed ionization energy of 30 eV are shown in Fig. 3. As the probe temperature was raised, the relative intensity tended to decline in the low mass windows less than $m/z = 400$, and the detectable peak range extended to higher *m*/*z* values, i.e., up to

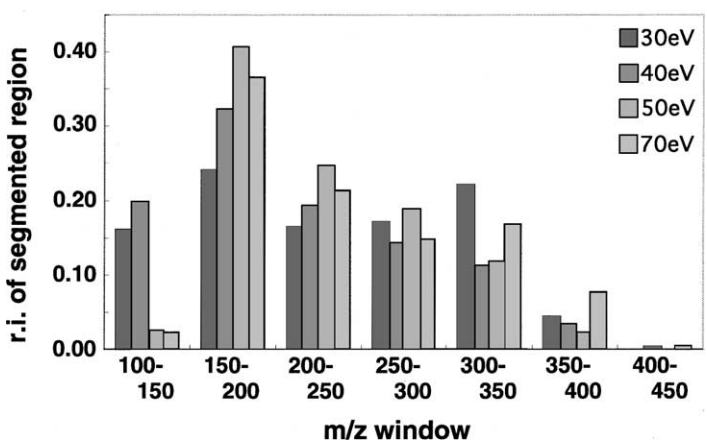

Fig. 2. Segmented mass spectrometric profile derived from Fig. 1.

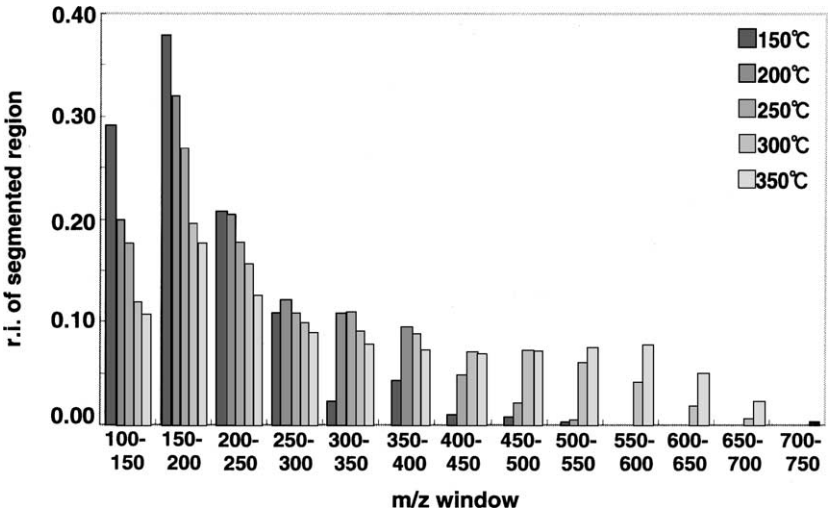

Fig. 3. Effect of probe temperature of in-beam EI on segmented mass spectrometric profile for AH-VR-Sa.

$m/z = 700$ at 350 °C. One of the possible reasons for the observed temperature dependency is that the amounts of constituents with low molecular weights would actually decrease with the higher probe temperature, because low molecular weight components had been vaporized already before the probe reached to the prescribed temperature. This may not be the case, since vacuum residue sample (AH-VR-Sa) consists of components with higher boiling point than 520 °C, which is much higher than the adopted probe temperature (350 °C). The most probable interpretation is as follows: the absolute abundance of the low mass constituents would not decrease, but the spectral distribution extended to the high mass region with the high probe temperature. This possibility is supported by an increase in the average molecular weight depending on a rise in the probe temperature as shown in Fig. 4. Recaluclating the relative intensity distribution for peaks in the range $100 < m/z < 300$, the intensity of every segmented window became independent of the probe temperature. Although the highest *m*/*z* peak was detected at 350 °C, the peak intensities over the whole detected range were maximized at 300 °C. Therefore, we decided to adopt 300 °C of the probe temperature and 30 eV of the ionization energy for molecular formula analysis of constituents.

Fig. 5 shows a wide-band spectrum of AH-VR-Sa obtained under the optimized ionization conditions: 300 °C of the probe temperature and 30 eV of the ionization energy. The peaks are found in the range of $100 < m/z < 700$. There are approximately 800 of distinguishable peaks and the presence of species is recognized at every nominal mass. All species are singly charged since there are no peaks between each nominal mass. In comparison with the previously reported application of EI FT-ICR MS to hydrocarbons [7] which were contained in petroleum and other refinery stream, the range of detectable peaks was extended up to *m*/*z* 700 by employing in-beam EI.

3.2. Molecular formula determination from accurate mass measurement

The mass scale expanded segment of Fig. 5 is shown in Fig. 6. The peak intensity pattern of the in-beam EI FT-ICR mass spectrum is significantly different from those of ESI FT-ICR mass spectra [10,12]. In the case of ESI, every peak with an even mass was more abundant than that with an adjacent odd mass across the whole detected range. Consequently, every peak with an odd mass in the ESI spectra was attributed to contain one ^{13}C. In contrast to the ESI case, the

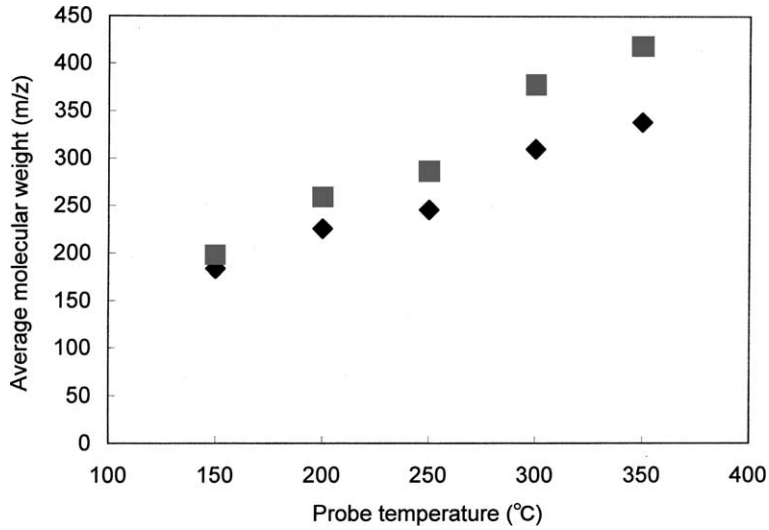

Fig. 4. Effect of probe temperature of in-beam EI on the average molecular weight for AH-VR-Sa. The number and weighted average molecular weight were denoted by (◆) and (■), respectively.

peak intensity ratio between odd and even masses in in-beam EI varies depending on the *m/z* values. For the peaks around $m/z = 316$, the peaks with even masses (no. 5 and 6) are more abundant than the adjacent peaks with odd masses (no. 7 and 8). On the contrary, the reverse order establishes for those around $m/z = 318$ (no. 9 and 10 vs. no. 11 and 12). The detailed mass analysis (see below) revealed that most of the distinguishable peaks (at both even and odd masses) in the in-beam EI spectrum were attributed

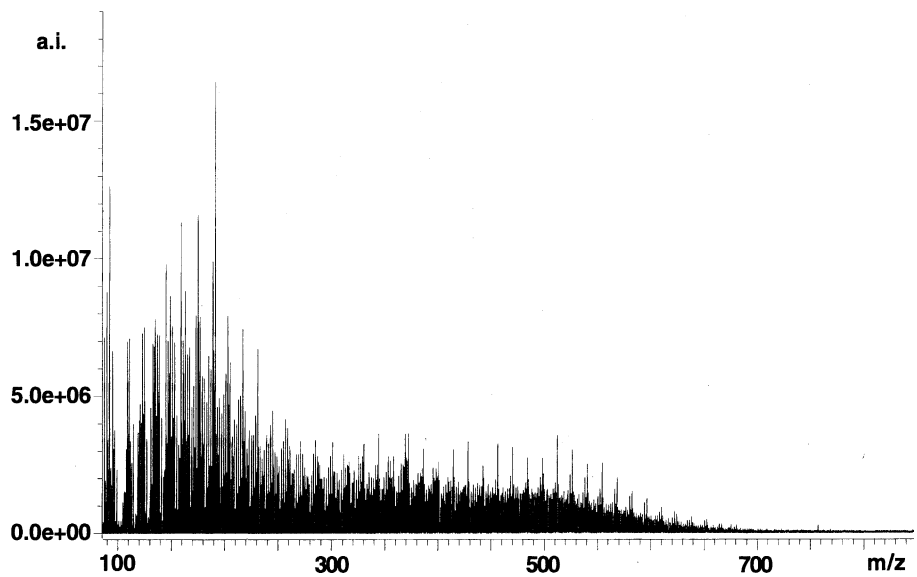

Fig. 5. Broad-band FT-ICR mass spectrum of AH-VR-Sa obtained in the optimized in-beam EI conditions; the probe temperature and the ionization energy were 300 °C and 30 eV, respectively.

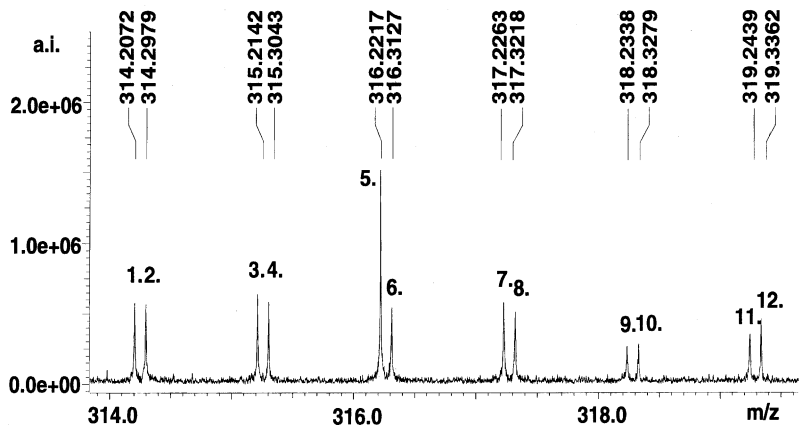

Fig. 6. Mass scale expanded segment of AH-VR-Sa mass spectrum shown in Fig. 5.

to monoisotopic (all ^{12}C) species. The presumable molecular formulas $[M]^+$ estimated by the accurate mass values for the peaks in Fig. 6 are summarized in Table 1, where the elemental composition is assumed to contain ^{1}H, ^{12}C, ^{32}S (less than 2) and ^{16}O (less than 2). The validity of the estimated molecular formulas $[M]^+$ was confirmed by using the Kendrick mass deficiency [15]. The deviations between the measured and the calculated mass values of the identified peaks are very small (0.1–1.9 mDa). The molecular formulas were determined for all the peaks observed in the whole mass range based on the accurate mass values. In petroleum analysis, it is common to categorize compounds by 'class,' i.e., the category based on the elemental compositions with the same content (e.g., S or O), and also by 'type,' i.e., the index based on the Z value defined by $C_nH_{2n+Z}S_sO_o$. The 'class' of the compounds detected in this spectrum were hydrocarbons with and without one sulfur atom ($[C_nH_{2n+Z}S]^+$ and $[C_nH_{2n+Z}]^+$, respectively) as major constituents and were hydrocarbons containing one-oxygen atom ($[C_nH_{2n+Z}O]^+$) as minor one. The compounds 'type' detected for each 'class' are discussed below.

3.3. Compound type distribution of C_nH_{2n+Z}

EI often yields $[M]^+$ ions of odd-electron spices in the positive ion mode. In Table 1, the estimated

Table 1
The estimated molecular formulas from accurate mass for the detected 12 peaks in Fig. 6

No.	Experimental mass (Da)	Estimated molecular formulas $[M]^+$	Theoretical mass	Error (mDa)	$m/\Delta m_{50\%}$
1	314.2072	$C_{21}H_{30}S$	314.2063	−0.9	40000
2	314.2979	$C_{23}H_{38}$	314.2968	−1.1	27000
3	315.2142	$C_{21}H_{31}S$	315.2141	−0.1	33000
4	315.3043	$C_{23}H_{39}$	315.3046	0.3	54000
5	316.2217	$C_{21}H_{32}S$	316.2219	0.2	51000
6	316.3127	$C_{23}H_{40}$	316.3125	−0.2	31000
7	317.2263	$C_{24}H_{29}$	317.2264	0.1	51000
8	317.3218	$C_{23}H_{41}$	317.3203	1.5	31000
9	318.2338	$C_{24}H_{30}$	318.2342	0.4	22000
10	318.3279	$C_{23}H_{42}$	318.3281	0.2	28000
11	319.2439	$C_{24}H_{31}$	319.2420	1.9	24000
12	319.3362	$C_{23}H_{43}$	319.3359	−0.3	40000

molecular formulas for the peaks with even masses (no. 2, 6, and 10) are $[C_nH_{2n+Z}]^+$ ions, and the peaks with odd masses (no. 4, 7, 8, 11, and 12) are $[C_nH_{2n+Z-1}]^+$ ions. For the molecular formulas originating from a peak with odd mass, Z value was defined as $[C_nH_{2n+Z\pm1}]^+$ to reflect its structure framework. Although there are two possible assignments for a peak with an odd mass: $[C_nH_{2n+Z+1}]^+$ from 'type' $Z = Z_0 - 2$ and $[C_nH_{2n+Z-1}]^+$ from 'type' $Z = Z_0$, the latter is more probable considering an estimated molecular formula which is attributed to the smallest species among the same compound 'type.' For instance, $m/z = 155.0857$ observed in Fig. 5 is assigned to be $C_{12}H_{11}$, which is the smallest molecular weight constituent in the series of this 'class' and 'type' (C_nH_{2n+Z-1}, $n \geq 12$, $Z = -12$) observable in the spectrum. Although $C_{12}H_{11}$ could be designated $[C_nH_{2n+Z+1}]^+$ from $Z = -14$ or $[C_nH_{2n+Z-1}]^+$ from $Z = -12$, it is difficult for $C_{12}H_{11}$ to have $Z = -14$ ($[C_nH_{2n-14+1}]^+$) because of its shortage in carbon number. Therefore, this class and type should be determined as $[C_nH_{2n-12-1}]^+$. This assignment suggests that most of the peaks with odd masses were fragment ions derived from larger species. The compound type distributions of C_nH_{2n+Z} for even masses and C_nH_{2n+Z-1} for odd masses are shown in Fig. 7. The 11 types with $Z = 2$ to -18 were found for hydrocarbon species (6 of 11 types are shown in Fig. 7) and the carbon numbers for the estimated molecular formulas ranged between 8 and 46. The maxima of peak intensities against the carbon number shifted to a larger carbon number with a decrease in the Z value.

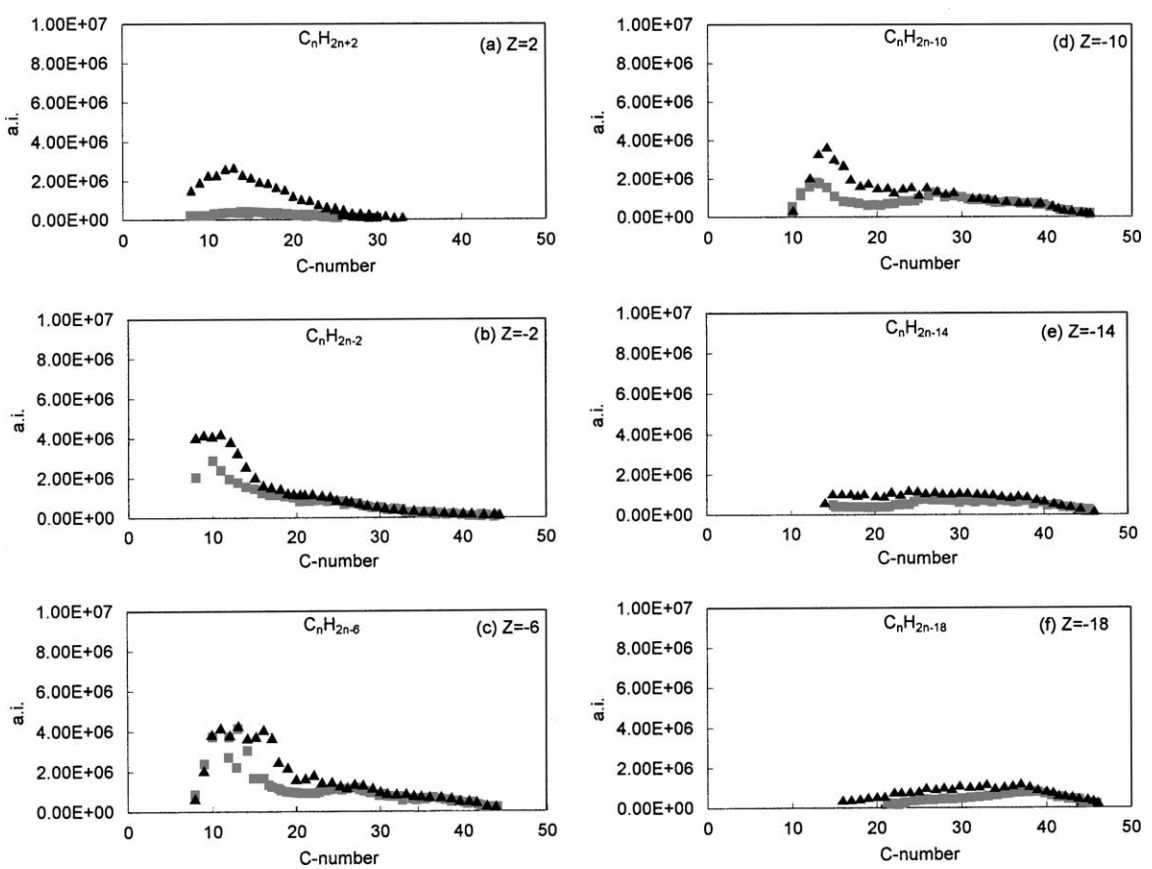

Fig. 7. Compound type distribution of C_nH_{2n+Z} estimated from Fig. 5: (a) $Z = 2$; (b) -2; (c) -6; (d) -10; (e) -14; (f) -18 (■, the peaks with even masses assigned to $[C_nH_{2n+Z}]^+$; ▲, the peaks with odd masses assigned to $[C_nH_{2n+Z-1}]^+$).

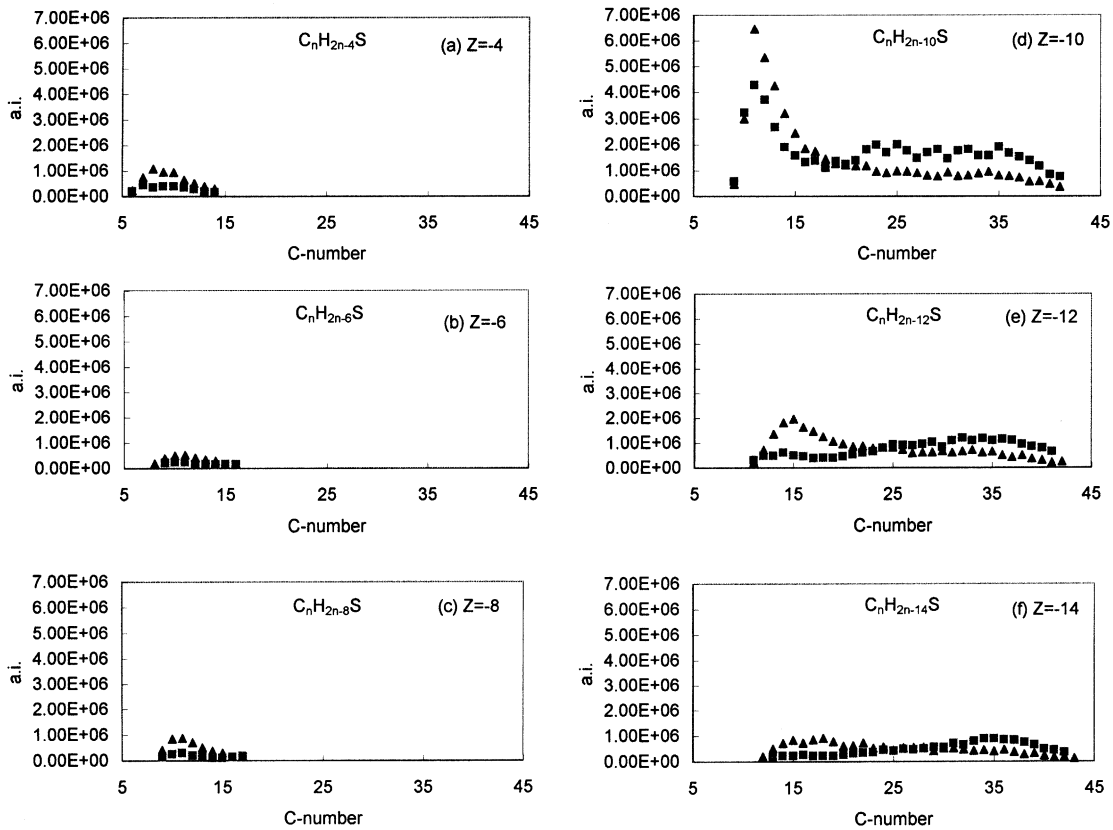

Fig. 8. The compound type distribution of $C_nH_{2n+Z}S$ estimated from Fig. 5: (a) $Z = -4$; (b) -6; (c) -8; (d) -10; (e) -12; (f) -14 (■, the peaks with even masses assigned to $[C_nH_{2n+Z}S]^+$; ▲, the peaks with odd masses assigned to $[C_nH_{2n+Z-1}S]^+$).

This insists that the degree of condensation of aromatic ring becomes higher as increasing in the molecular weight. In general, the peak intensities of every odd (▲) and even (■) masses having the same compound types and carbon numbers over 30 are approximately the same. The significant discrepancy was observed for the peaks with carbon numbers less than 20 and relatively high Z values, where the intensities of peaks with odd masses (▲) were higher than those with even ones (■). The compounds in this region are thought to be mostly aliphatic by considering the high Z value and the carbon number. One of possible reasons for the observed abundance of the odd masses is a contribution of $[C_nH_{2n+Z}S]^+$ ions (described later), which can generate fragment ions originating from their aliphatic side-chains without sulfur atom.

3.4. Compound type distribution of $C_nH_{2n+Z}S$

Fig. 8 shows compound type distributions of $C_nH_{2n+Z}S$ estimated on the basis of the peaks observed in Fig. 5 by the similar manner for the hydrocarbon compounds. The detected compounds with one sulfur atom ranged of $Z = -4$ to -16 and of the carbon numbers 6–44. Comparing to the detected hydrocarbon species ($Z = 2$ to -18) shown in Fig. 7, the distribution of Z value is narrow. Compounds

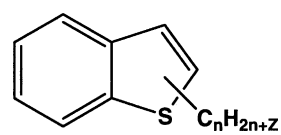

Fig. 9. A presumable structure for $C_nH_{2n-10}S$.

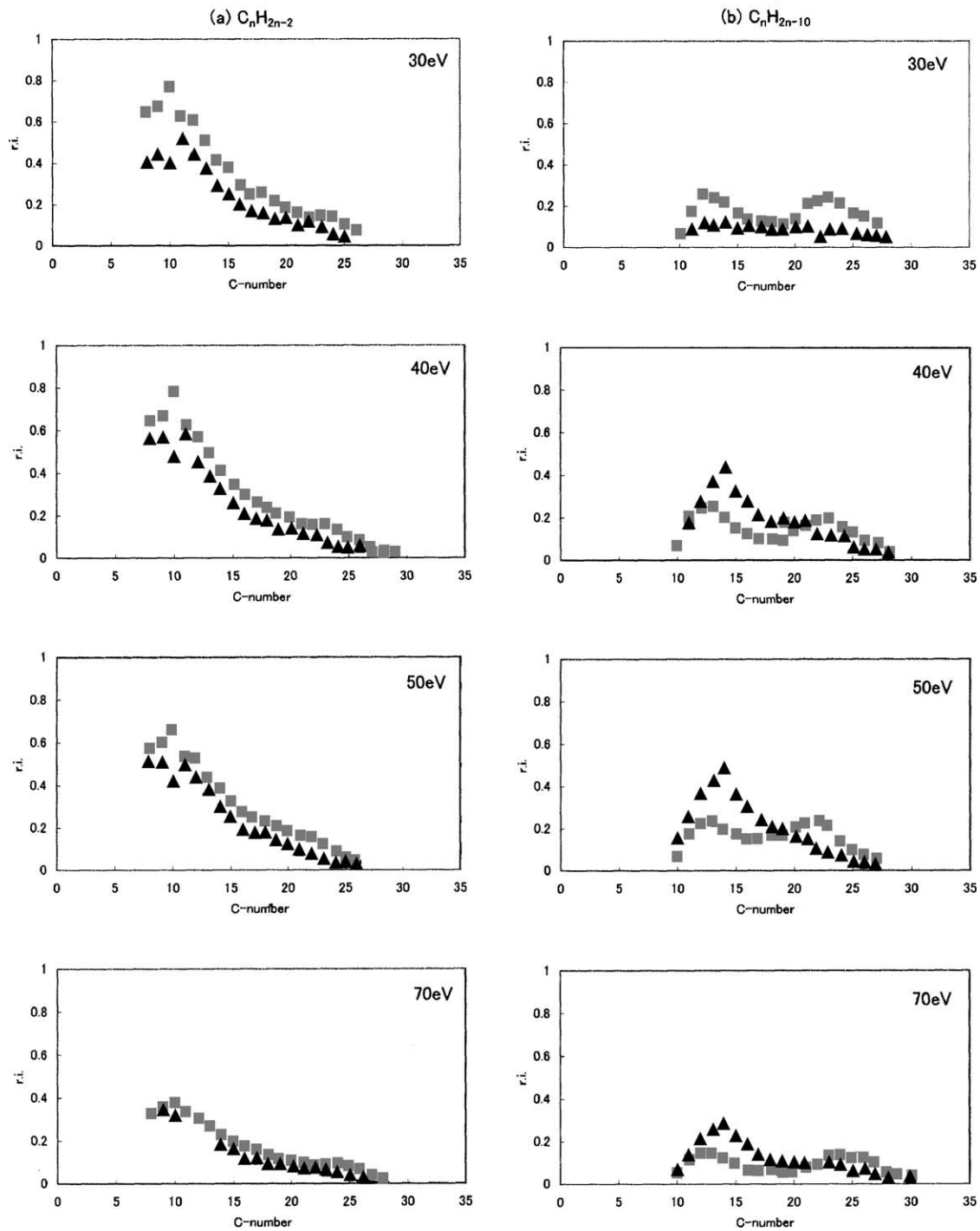

Fig. 10. The effect of compound type (C_nH_{2n+Z}, or $C_nH_{2n+Z}S$) distribution on the ionization energy. (a) C_nH_{2n-2} ($Z = -2$), (b) C_nH_{2n-10} ($Z = -10$), (c) $C_nH_{2n-4}S$ ($Z = -4$) and (d) $C_nH_{2n-10}S$ ($Z = -10$) (■, the peaks with even masses; ▲, the peaks with odd masses).

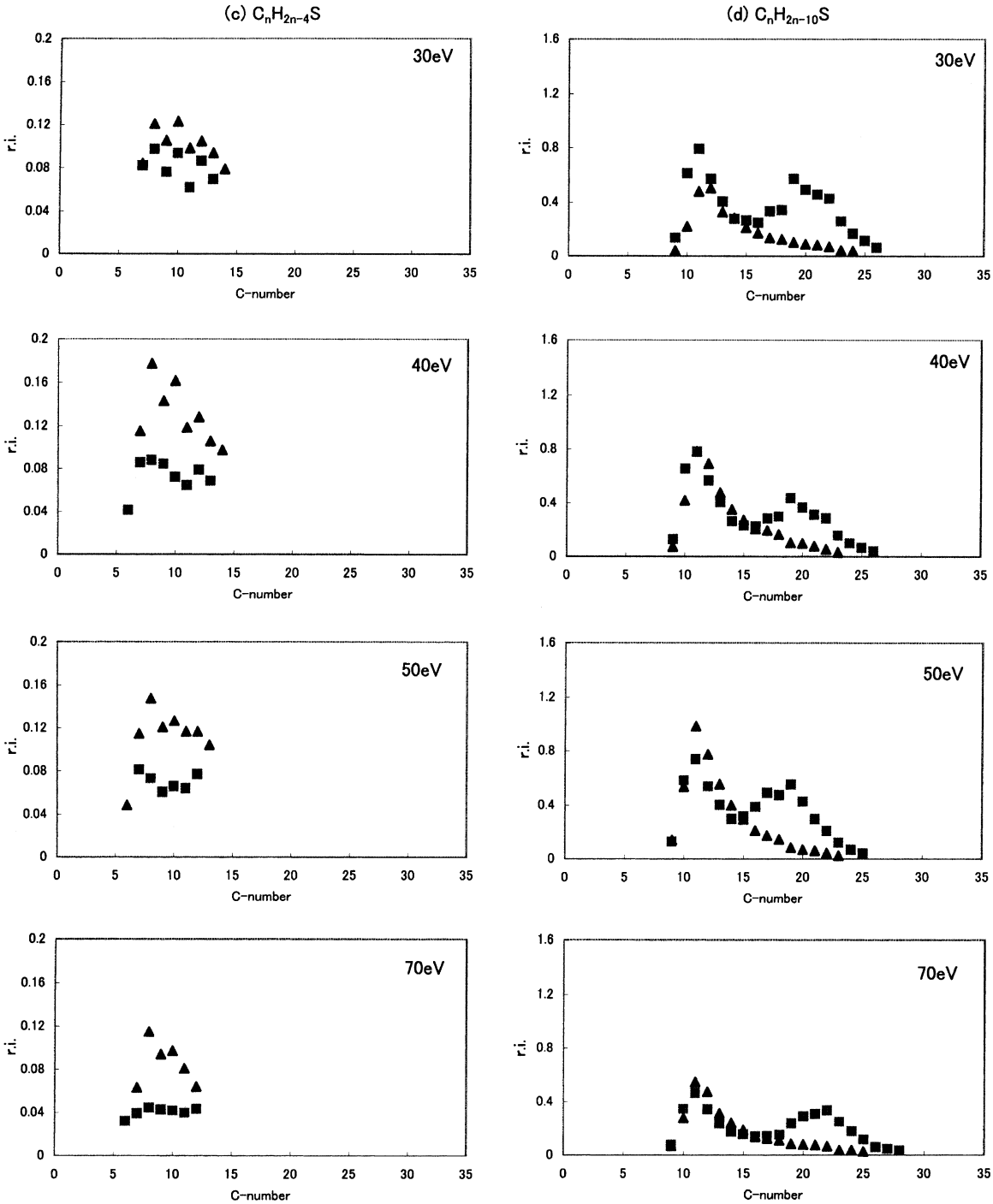

Fig. 10. (*Continued*).

correspond to aliphatic sulfur compounds with $Z = 2$ to -2 were not detected in the present study, even at the ionization energy of 70 eV. This result indicates that there is no sulfur atom located in an aliphatic component which should be detected as fragment peaks with $Z = 2$ to -2 if exist. Most of the sulfur atoms therefore may be located at an aromatic ring. Among compounds containing one sulfur atom, species with $Z = -10$ was the most abundant for every number of carbons. A presumable structure of this type is shown in Fig. 9. The detection of such compound is consistent with the result obtained in low voltage electron ionization mass spectrometry (LVEI MS) of a thermally cracked petroleum distillate reported by Qian and Hsu [17]. One of the remarkable differences in the type distributions between 'with' and 'without' one sulfur atom shown in Figs. 7 and 8 are the dependence of the detectable carbon numbers on the Z value. The detected carbon numbers of the sulfur compounds with $Z = -4$ to -8 were limited less than 17. A common trend, i.e., type distribution shifts to smaller carbon number with increasing in the Z value, was also observed in hydrocarbons; however, the maximum carbon number detected was limited to low value for the sulfur compounds. In Fig. 8, the peaks with odd masses which originate from fragment ions are more abundant than those with even masses when the carbon numbers of the estimated molecular formulas are below ca. 20.

3.5. Effect of the ionization conditions on the detected compound type

The effects of the ionization energy and the probe temperature on the compound type distribution were explored. The detected constituents were classified according to the Z value and either with or without sulfur atom (Fig. 10). In the ionization energies of 40 eV and higher, the intensities of fragment peaks with odd masses were higher than those of molecular ion peaks with even masses for every compound type in low carbon number region, except the hydrocarbons with $Z = -2$. This result and Fig. 7 indicate that fragmentation was minimized at 30 eV in our measurements. Single-mode distributions were obtained for the relative intensities against the number of the carbons in the hydrocarbons with $Z = -4$ and more ($Z = -2$ is shown in Fig. 10). These distributions have stretched shoulders toward higher carbon numbers and the maximum values at C_{10}. The distributions for the hydrocarbons with $Z = -6$ and less ($Z = -10$ is shown in Fig. 10) were bimodal with mode values of C_{13} and C_{23}. These mode values did not change for 30, 40, 50 eV and became slightly higher only at 70 eV, although the detectable carbon number of compounds became higher as raising the ionization energy. The distributions of the compounds containing one sulfur atom were similar to those of the hydrocarbons irrespective of the ionization energy. The probe temperature also didn't affect the compound type distribution. The bimodal distributions became more apparent when the compound type distributions were sorted by the ionization energy. These distributions were observed depending on the Z-number of constituents. The hump in low mass region may mainly consist of aliphatic constituents and fragment ions, and the hump in high mass region may consist of the constituents with low Z numbers.

4. Conclusion

In conclusion, we demonstrated that in-beam EI FT-ICR MS is a viable tool for analysis of a vacuum residue and revealed that the *n*-heptane-soluble fraction separated from AH-VR is able to be ionized by in-beam EI in contrast to ESI. Through exploring preferable experimental conditions, it was indicated that the average molecular weight increased only dependent upon the probe temperature while both the ionization energy and the probe temperature affected a distribution of detected peaks. This fact suggests that the high ionization energy tends to cause the fragmentation more seriously than the high probe temperature. The current probe system has a temperature limitation up to 350 °C; however, in-beam EI effectively extended the range of AH-VR-Sa peaks toward a higher m/z.

Molecular formulas of components contained in AH-VR-Sa were determined simply by the accurate mass measurements. Hydrocarbons with and without one sulfur atom were detected as major constituents in AH-VR-Sa. The detectable compound 'types' by in-beam EI were the species with larger Z values than those ionized by ESI. This finding suggests that in-beam EI can be used as complementary to ESI for analysis of vacuum residues. The compounds with $Z = -10$ were the most abundant constituents for sulfur-containing species, irrespectively on their carbon numbers. Our result insists that a sulfur atom is located in an aromatic framework but not in a side chain for most of the sulfur-containing species.

References

[1] M.M. Boduszynski, Energy and Fuels 2 (1988) 597.
[2] S. Asaoka, S. Nakata, J. Jpn. Inst. Energy 65 (1986) 783.
[3] H.E. Lumpkin, Anal. Chem. 36 (1964) 2399.
[4] E.J. Gallegos, J.W. Green, L.P. Linderman, R.L. Letourneau, R.M. Teeter, Anal. Chem. 39 (1967) 1833.
[5] T. Aczel, Rev. Anal. Chem. 1 (1972) 226.
[6] C.S. Hsu, Z. Liang, J.E. Campana, Anal. Chem. 66 (1994) 850.
[7] S. Guan, A.G. Marshall, S.E. Scheppele, Anal. Chem. 68 (1996) 46.
[8] R.P. Rodgers, F.M. White, C.L. Hendrickson, A.G. Marshall, Anal. Chem. 70 (1998) 4743.
[9] M. Ohashi, K. Tsujimoto, S. Funakura, K. Harada, M. Suzuki, Spectrosc. Int. J. 2 (1983) 260.
[10] K. Miyabayashi, K. Suzuki, T. Teranishi, Y. Naito, K. Tsujimoto, M. Miyake, Chem. Lett. (2000) 172.
[11] K. Miyabayashi, Y. Naito, K. Tsujimoto, M. Miyake, Eur. Mass Spectrom. 6 (2000) 172.
[12] K. Qian, R.P. Rodgers, C.L. Hendrickson, M.R. Emmett, A.G. Marshall, Energy and Fuels 15 (2001) 492.
[13] G.J.V. Barkel, S.A. McLuckey, G.L. Glish, Anal. Chem. 64 (1992) 1586.
[14] G.J.V. Barkel, K. Asano, Anal. Chem. 66 (1994) 2096.
[15] E. Kendrich, Anal. Chem. 35 (1963) 2146.
[16] E.Y. Sheu, Energy and Fuels 16 (2002) 74.
[17] H. Qian, C.S. Hsu, Anal. Chem. 64 (1992) 2327.